Available online at BCREC Website: http://bcrec.undip.ac.id

Bulletin of Chemical Reaction Engineering & Catalysis, 10 (3), 2015, 237-248

Research Article

Modified Zeolite with Transition Metals Cu and Fe for Removal of Methylene Blue from Aqueous Medium: Mass Spectrometry Study

João Henrique Lopes[1,*], Francisco Guilherme E. Nogueira[2], Maraísa Gonçalves[2], Luiz Carlos Oliveira[2]

[1] Institute of Chemistry, University of Campinas, P.O. Box 6154, CEP 13083-970 Campinas, São Paulo, Brazil

[2] Department of Chemistry, Federal University of Lavras, P.O. Box 3037, CEP 37200-000, Lavras, Minas Gerais, Brazil

Received: 4th June 2015; Revised: 29th July 2015; Accepted: 29th July 2015

Abstract

Textile industries are one of the main sources of water pollution. Wastewater containing dyes present a serious environmental problem because of its high toxicity and possible accumulation in the environment. In this work were explored the characteristics of removal of methylene blue dye employing zeolites modified with transition metals (Cu, Fe). The zeolites with iron or copper were prepared by using NaY and Naβ zeolites as precursors, replacing part of ion sodium for copper or iron ions through the ion exchange method. All materials were characterized by several analytical techniques, in order to gain information about the structure and catalytic activity. Modified zeolites showed a remarkable activity in H_2O_2 decomposition and in the discoloration an organic dye in aqueous medium. ESI-MS studies of the methylene blue oxidation showed that the oxidation of the dye occurs via a Fenton type system in which *OH radicals are formed in situ and added to the ring structure of the organic substrate. In addition, modification of the zeolite with transition metal proved to be an interesting pathway to produce efficient catalysts for the oxidation of organic molecules, i.e. dyes in aqueous media.

Keywords: Y zeolite; β zeolite; ion exchange; removal of organic contaminant; oxidation reactions

How to Cite: Lopes, J.H., Nogueira, F.G.E, Gonçalves, M., Oliveira, L.C. (2015). Modified Zeolite with Transition Metals Cu and Fe for Removal of Methylene Blue from Aqueous Medium: Mass Spectrometry Study. *Bulletin of Chemical Reaction Engineering & Catalysis*, 10 (3): 237-248. (doi:10.9767/bcrec.10.3.8624.237-248)

Permalink/DOI: http://dx.doi.org/10.9767/bcrec.10.3.8624.237-248

1. Introduction

Textile industries consume large volumes of water and chemicals for wet processing of textiles. There are more than 100,000 commercially available dyes with over $7x10^5$ ton of dye produced annually [1]. Wastewater containing dyes present a serious environmental problem because of its high toxicity and possible accumulation in the environment [2-4]. The removal of textile dyes from wastewater is one of the most important environmental issues to be solved today [5-7]. Several dyes used in the textile industry are particularly difficult to remove with conventional waste treatment methods since they are designed to be resistant to degradation [4, 8, 9].

* *Corresponding Author.*
E-mail: henriquelopez@gmail.com (J.H. Lopes)
Phone: +55-19-35213036, Fax: +55-19-35213023

New and innovative methods are of great importance to devise technologies for dealing with environmental problems [10]. The application of modified catalyst technology to solve environmental problems is one of these methods that have received considerable attention in recent years [11, 12]. The zeolites can be modified according to various strategic forms to improve their activity and catalytic selectivity [13, 14]. The zeolite modification by the introduction of transition metals causes the zeolite to present activity mechanisms comparable to those found in enzymes [15].

Acid solids are the most used catalytic material in the petrochemical industry. Among them, the zeolites have become extremely important for innumerable processes, such as oil refining, catalytic cracking of long hydrocarbons for high-octane gasoline, supports, gas separation, water treatment and production of fine chemical products [16, 17].

The present work aims to investigate two zeolites supports, Y and *β*, both modified with iron or copper as catalyst for the degradation of the organic compound methylene blue dye in presence of hydrogen peroxide.

2. Materials and Methods

2.1. Modification of NaY and Na*β* Zeolites

In the present experiment, NaY (Si/Al = 2.8) and Na*β* (Si/Al = 20) zeolites were supplied by the Chemical Institute of Technology in Valence, Spain. Solids precursors were converted to active catalysts by ion exchange [18, 19]. Adsorbents NaY and Na*β* were ion-exchanged using 5 g of each zeolite with 200 ml of copper nitrate 265 mmol.L^{-1} or solution of iron nitrate 278 mmol.L^{-1}. The mixture was stirred for 24 h at room temperature (25 ^{o}C). The powders were filtered and washed until the filtrate was metallic ion free. Thereafter, the pH of the mixture was raised to 7.5 with ammonium hydroxide 3 mol.L^{-1}, leaving under stirring for a further 1 hour. The remaining material was filtered and dried at 110 ^{o}C for 24 h and calcined in a muffle furnace using a heating rate 5 ^{o}C min^{-1} at 500 ^{o}C for 3 h in air followed by 2 h under H_2 atmosphere. The prepared materials were labeled as Y-Fe, Y-Cu, *β*-Fe and *β* -Cu.

2.2. Characterization of the Materials

The textural properties of the Y-Fe, Y-Cu, *β*-Fe and *β*-Cu samples were determined by N_2 adsorption and desorption isotherms at -196 ^{o}C using a surface area measurement analyzer (Micromeritics ASAP-2000, Micromeritics Instrument Corporation, Norcross, Georgia, USA). The sample was degassed for 24 h at 110 ^{o}C prior to the adsorption and desorption analysis. The BET surface area (S_{BET}) and total pore volume (V) of the zeolites were obtained from

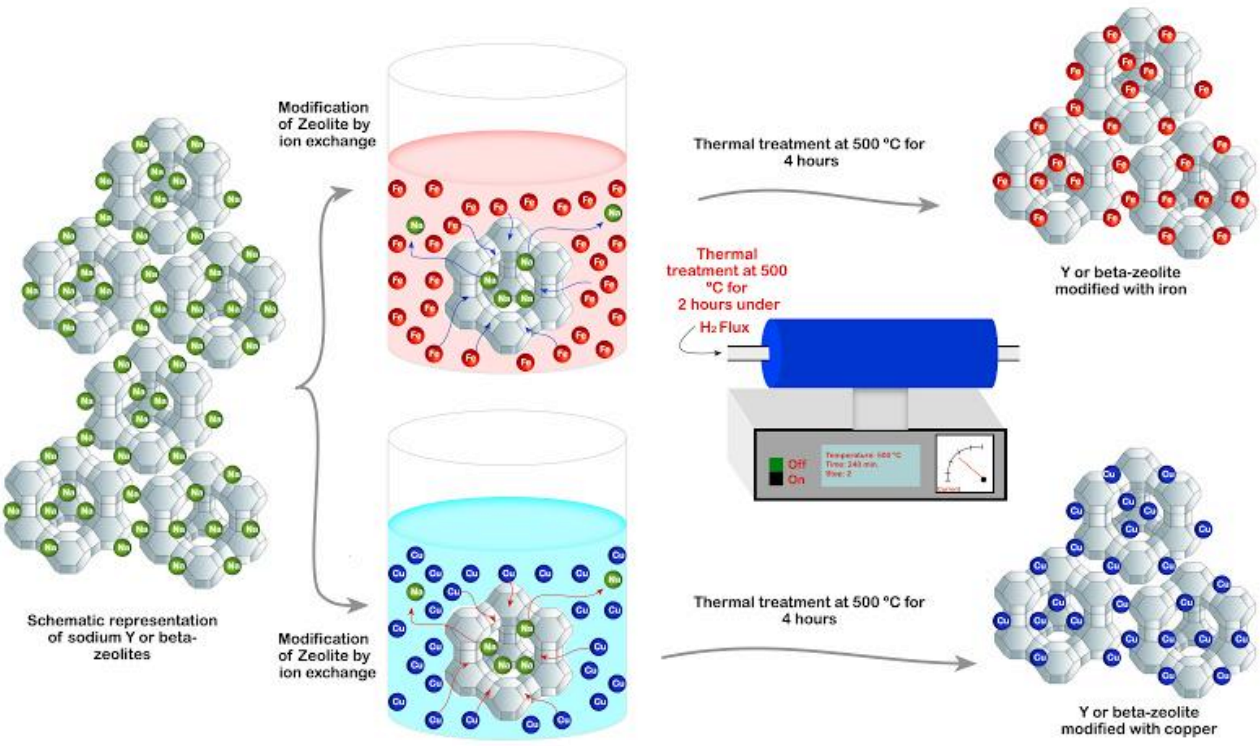

Figure 1. Representative scheme summarizing all steps carried out in this work.

the adsorption/desorption isotherms.

The samples were analyzed also by X-ray diffractometry (Shimadzu 7000 diffractometer, Shimadzu Corporation, Tokyo, Japan) using the Bragg Brentano camera geometry and the Co-K_α incident radiation (λ = 1.5418 A), 40 kV, 30 mA and acquisition rate of 2º min^{-1} between 10-60º (2θ) range.

The transmittance spectra were collected using an interferometric spectrometer (MB-102, ABB Bomem Inc., Quebec, Canada). KBr pellets were prepared by mixing 1 mg of bioglasses powders with 100 mg of KBr. FTIR spectra were acquired in the region 4000-400 cm^{-1} with spectral resolution of 4 cm^{-1} and 64 scans.

Temperature programmed reduction (TPR) technique was performed using a semi-automated analyzer (Chemisorption - Chem-BET® 3000 TPR/TPD, Quantachrome Instruments, Boynton Beach, FL, USA). TPR experiments were performed using 20 mg of sample was loaded into a U-shaped quartz micro reactor (2 mm internal diameter) and then pre-treated in a flow of He (40 $ml.min^{-1}$) at 400 °C for 0.5 h. After the sample was cooled down to room temperature in He, the reduction of the sample was carried out from 30°C to 500°C in a flow of 5 % H_2/N_2 (27 $ml.min^{-1}$) at a heating rate of 10 °$C.min^{-1}$. The consumption of H_2 was monitored continuously by a thermal conductivity detector. The water produced during the reduction was trapped in a 5A molecular sieve column. Figure 1 shows a representative scheme summarizing all steps carried out in this work.

2.3. Oxidation Reaction

Two reactions were performed in the presence of the Y-Fe, Y-Cu, β-Fe and β -Cu samples: (i) the H_2O_2 decomposition to O_2 in water and (ii) the oxidation of the dye methylene blue. For the first, a typical decomposition of hydrogen peroxide was carried out: 2 ml of H_2O_2 solution (30% v/v) with 5 ml of H_2O and 30 mg of the composite magnetically stirred and monitored by measuring the formation of gaseous O_2 in a volumetric glass system. The activity of the zeolites was tested for their effectiveness in discoloring the methylene blue dye in water (10 ml of a 100 $mg.L^{-1}$ solution) by using 10 mg of the material in presence of hydrogen peroxide. The dye decomposition was measured at 665 nm with an UV/Vis spectrophotometer (UVPC 1600, Shimadzu Corporation, Tokyo, Japan). All reactions were performed at room temperature 25 ºC.

2.4. Studies by ESI-MS

In an attempt to identify the intermediate formation, the methylene blue decomposition was monitored with electrospray ionization mass spectrometry (ESI-MS) in the positive ion mode in an ion trap mass spectrometer (Agilent 6300 Ion Trap LCMS, Santa Clara, California, USA). The reaction samples were analyzed by introducing aliquots into the ESI source via a syringe pump at a flow rate of 5 $\mu L \cdot min^{-1}$. The spectra were obtained as an average of 50 scans, each for 0.2 s. Typical ESI conditions were as follows: heated capillary temperature, 250 ºC; heath gas (N_2) flow rate, 20 units (4 $L.min^{-1}$); spray voltage 4 kV; capillary voltage 25 V; tube lens off set voltage, 25 V.

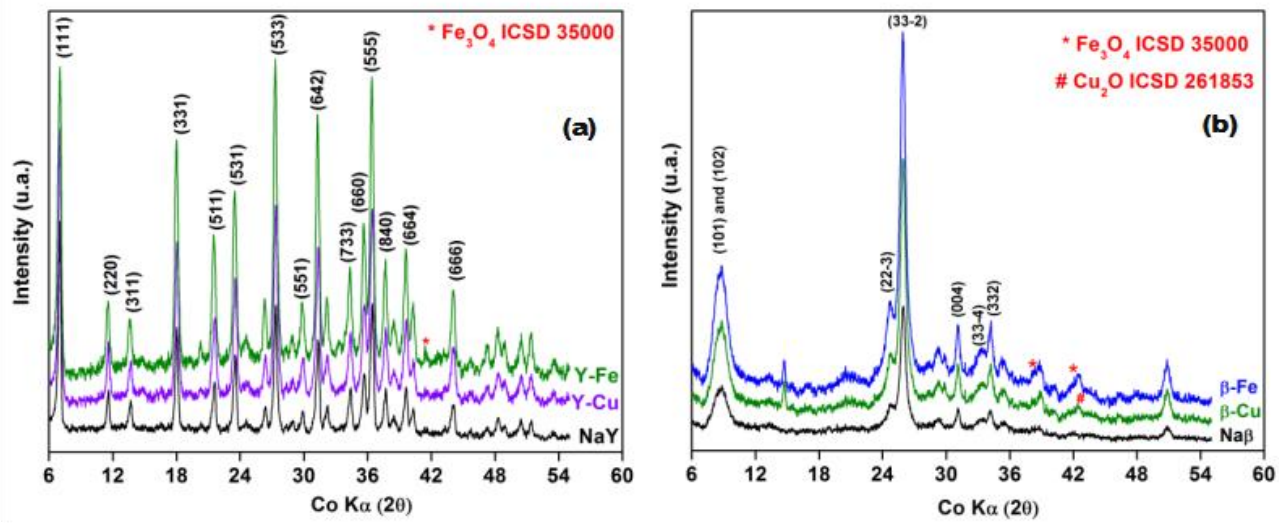

Figure 2. XRD patterns of precursors and modified zeolites with copper and iron: (a) NaY, Y-Cu, Y-Fe and (b) Naβ, β-Cu, β-Fe

3. Results and Discussion

3.1. Characterization of the Materials

The effects of acid activation on the zeolites surfaces are clearly seen in the scanning electron micrographs (SEM) of precursors and modified zeolites (supplementary materials, Figure SM-1). The analysis of the diffraction patterns for the pre cursors samples NaY and Naβ (see Figure 2a and 2b) indicated excellent fit with the standard Inorganic Crystal Structure Database (ICSD) Collection Code ICSD 34807 [20] and ICSD 97105 [21], corresponding typical structures of the sodium Y and sodium β zeolites, respectively [22].

Regarding to the modified Y zeolite the occurrence of specific diffraction peaks characteristic of crystalline phases associated with copper or iron in the Y-Cu and Y-Fe samples is unclear (Figure 2a). These results may be related to the small size of the formed particles and/or high dispersion of these on the surface and/or in the pore walls of zeolites, which would not be easily observed by XRD analysis. The corresponding XRD patterns of β-Cu and β-Fe samples (Figure 2b) showed subtle changes compared to the β zeolite which can be assigned to the Cu_2O (ICSD 261853) [23] and Fe_3O_4 [24], respectively.

Fourier transform infrared (FTIR) spectra of zeolites are shown in Figure 3. The characteristic peaks of at ~3440 cm^{-1} and ~1640 cm^{-1} are corresponding to the OH-stretching vibration and the signal stretching and angular deformation of the hydroxyl molecules of water of hydration of the zeolites, respectively. The absorptions set in the region between 900 and 1300 cm^{-1} are related to the overlapping of several absorptions related to asymmetric stretching the Si-O in Si-O-Si and Si-O-M (M= Al, Fe or Cu) groups [25]. Also in this spectral region are contained all absorptions regarding the Si-OH and Al-OH species [26]. The region between 700 and 900 cm^{-1} exhibits a single and weak absorption at ~790 cm^{-1} for materials based on β zeolite and several small absorptions (more intense at ~790 and ~710 cm^{-1}) for derived materials from Y zeolite. These spectral features are attributed to overlapping of Si-O bending mode in Si-O-Si and Si-O-M (M= Al, Fe or Cu) groups [27]. Lower frequencies (400-700 cm^{-1}) are localized the symmetric stretch vibrational modes of Si-O-Si and Si-O-Al groups where the Al is in octahedral coordination [26], stretching of Fe-O in magnetite crystal phase [27], stretching of Cu-O at ~525 cm^{-1}, and CuO nanostructures at ~580 cm^{-1} [28].

Figure 4 shows the profiles obtained by reduction of the temperature programmed reduction (TPR) to the zeolite before and after the process of ion exchange with Cu and Fe. TPR analysis for NaY zeolite precursor did not show any signal in the curve (Figure 4a), indicating the absence of species capable of undergoing reduction conditions employed in the analysis. In the temperature range studied, the TPR profile of Cu-Y shows a single reduction peak, broad and centered at 284 °C. This signal is related to the reduction of Cu^{2+} to Cu^{+} from isolated species [29] and reduction of Cu^{2+} to Cu^{0} from CuO species [30], according to Equations (1-2):

$$CuO + H_2 \rightarrow Cu_2O + H_2O \quad (1)$$

$$Cu_2O + H_2 \rightarrow Cu^0 + H_2O \quad (2)$$

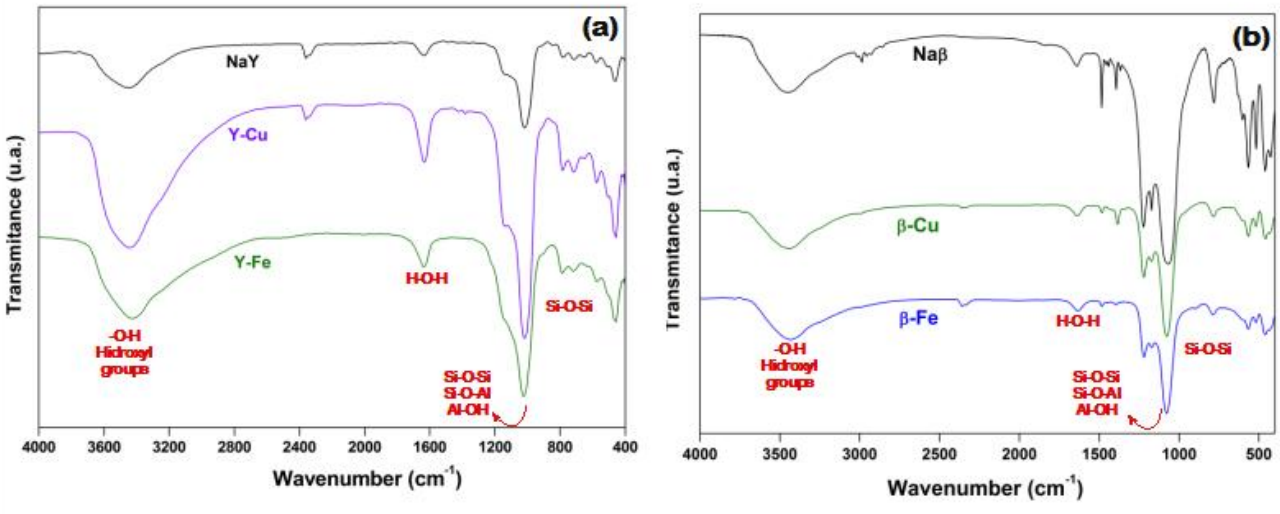

Figure 3. Infrared spectra of precursor and modified zeolites with copper and iron: (a) NaY, Y-Cu, Y-Fe and (b) Naβ, β-Cu, β-Fe

For Y-Fe zeolite was observed a complex reduction profile with three well-defined peaks: one centered at 424 ºC, a second peak more intense centered at 496 ºC and the third peak, the wider, with maximum at 593 ºC. These peaks are likely related to iron oxide formed onto the Y-Fe zeolite. These results are in agreement with TPR studies of iron oxide-pillared clays in the literature which suggest that the reductions occurring at approximately 400 ºC are due to the partial reduction of Fe^{3+} to produce Fe_3O_4 [31] and complete reduction for Fe^{2+} [18], according to Equations (3-4), respectively:

$$3Fe_2O_3 + H_2 \rightarrow 2Fe_3O_4 + H_2O \quad (3)$$
$$Fe_3O_4 + H_2 \rightarrow 3FeO + H_2O \quad (4)$$

At higher temperatures, the FeO is reduced to Fe^0 [18], according to Equation (5):

$$FeO + H_2 \xrightarrow{\sim 590\ ^oC} Fe0 + H_2O \quad (5)$$

For zeolites Naβ was not observed the presence of any signal consumption of H_2, nevertheless a negative signal was observed at 460 °C (Figure 4b). This signal may be attributed to support decomposition or desorption of H_2 adsorbed inside the pores of zeolite, which would be someway trapping the H_2 molecules. As the temperature is increased occurs the transfer of thermal energy to the molecules H_2, reaching a threshold value, which promotes desorption and a negative sign in the TPR curve. For the β-Cu sample, it is possible to notice a region of H_2 consumption very broad, centered at 169 and 296 ºC. These peaks reduction are associated with changes in the oxidation state of Cu^{2+} to Cu^+ from isolated species [29] and Cu^{2+} to Cu^0 from CuO species [30] (see Equations (1) and (2)). On the other hand, for the β-Fe desorption of H_2 molecules within the pores of zeolites overshadowed signal reduction referring to Equations (3-4), leaving only one reduction broad peak at high temperature (556 ºC) related formation of Fe^0 (see Equation (5)). TPR results show that the thermal treatment under a hydrogen atmosphere was not enough to produce a complete reduction of the iron or copper species, but only a partial reduction.

The N_2-adsorption measurements of the NaY, Y-Fe, Y-Cu and Naβ, β-Fe and β-Cu samples are shown in Figure 5a and b, respectively. Table 1 summarizes the specific surface area BET and porosity values for NaY, Y-Fe, Y-Cu, Naβ, β-Fe and β-Cu samples.

In both supports, NaY and Naβ, the BET surface areas decreased after the sodium replacement within the host materials by Cu or Fe. There are two main factors that may affect the surface area: the size and the number of compensating cations [32]. Copper and iron have different charge of sodium and the ionic radius of the Cu^{2+} and $Fe^{2+/3+}$ are smaller than Na^+. Thus, it would be expect to observe an effect inverse on the surface area behavior. However, the influence on surface area for multivalent cations is very complex. For these ions, not only the size, but also their configurations and their total number in the framework are parameters very important and must be considered [32]. The Na^+ ion is larger than Cu^{2+} or $Fe^{2+/3+}$ ions, thus more than one Cu or Fe are occupying each Na+ ion site. Strictly speaking, every Na^+ site is offset by cluster of Cu or Fe after ion exchange, assuming an exchange degree of 100%. It fills part of the pores of the pores reducing its vol-

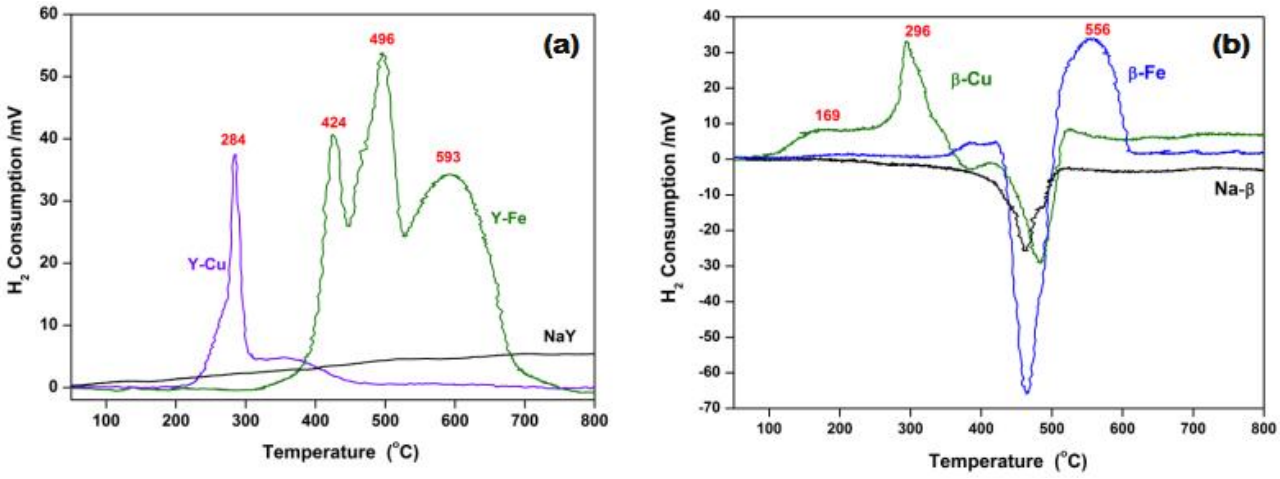

Figure 4. TPR analyses for of precursor and modified zeolites with copper and iron: (a) NaY, Y-Cu, Y-Fe, and (b) Naβ, β-Cu, β-Fe

ume and thus decreasing the total surface area (see Table 1 and Figure 6).

3.2. Catalytic Tests

The catalytic activity of the zeolites was studied using two reactions: (i) the H_2O_2 decomposition to O_2 ($H_2O_2 \rightarrow H_2O + 0.5O_2$); (ii) the oxidation of the model contaminant the methylene blue dye with H_2O_2 in aqueous medium. Figure 7a shows the performance of materials in the H_2O_2 decomposition.

Kinetics study of the oxidation reaction of hydrogen peroxide in the presence of NaY, Na-β, and Y-Fe zeolites showed that the H_2O_2 concentration remains constant, indicating that these materials are not able to catalyze the decomposition of peroxide in the studied conditions. Conversely, kinetics study in the presence of β-Fe, β-Cu, and Y-Cu reveal a linear dependence between the decreases of H_2O_2 concentration with the increase of reaction time. This behavior for β-Fe, β-Cu, and Y-Cu zeolites show that although the H_2O_2 decomposition is a complex reaction, the linear dependence of the decomposition curves between 5 and 20 min suggests that the process can be approximate to pseudo-zero order kinetics. The quick decomposition of H_2O_2 in the first 5 minutes of reaction for β-Fe, β-Cu, and Y-Cu zeolites reveals a high catalytic activity for the H_2O_2 oxidation that is very interesting in Fenton-type reactions. Furthermore, Y-Cu showed a catalytic activity slightly higher than that observed for the β-Cu or β-Fe samples. The distinct behavior exhibited by β-Cu and Y-Cu in the H_2O_2 decomposition reaction is related to reduced copper species present in the phases formed in the modified zeolite. In addition, the reduction of Cu(II) by H_2O_2 (4.6×10^2 $M^{-1}.s^{-1}$) occurs more easily than that of Fe(III), and the Cu(I)-H_2O_2 system, which possesses a higher reaction rate (1×10^4 $M^{-1}.s^1$) than the Fe(II)-H_2O_2 system (76 $M^{-1}.s^1$), can efficiently produce *OH [33].

Table 1. BET surface area (S_{BET}), total pore volume ($V_{total\ 0.95}$), micro (V_{micro}) and mesopore (V_{meso}) volumes for precursors (NaY and Naβ) and modified zeolites with copper (Y-Cu, β-Cu) and iron (Y-Fe, β-Fe).

Sample	Surface area BET /$m^2.g^{-1}$	$V_{total\ 0.95}$ $cm^3.g^{-1}$	V_{micro} $cm^3.g^{-1}$	V_{meso} $cm^3.g^{-1}$
Naβ	206	0.35	0.11	0.25
β-Cu	187	0.30	0.10	0.20
β-Fe	119	0.23	0.06	0.17
NaY	737	0.31	0.30	0.01
Y-Cu	720	0.31	0.29	0.02
Y-Fe	539	0.23	0.21	0.02

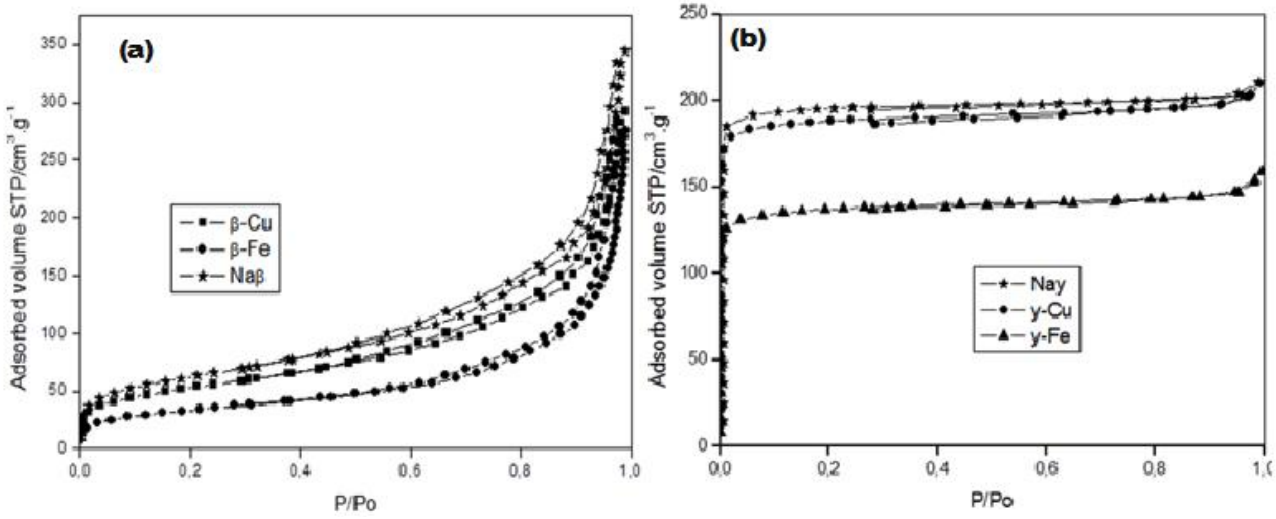

Figure 5. Adsorption/desorption isotherms N_2 77 K for of precursors and modified zeolites with copper and iron: (a) NaY, Y-Cu, Y-Fe and (b) Naβ, β-Cu, β-Fe

The heterogeneous Fenton reactions were carried out using the dye methylene blue as probe molecule. The reaction kinetics was investigated by UV/Vis discoloration measurements (Figure 7b) to form non-colored intermediates and the oxidation efficiency was measured by ESI-MS as showed in Figure 8.

In the control experiment (only methylene blue and H_2O_2 but no zeolite) there is no significant discoloration even after 120 min. of reaction time (not shown here). On the other hand, in the presence of the zeolite supports Naß and NaY a slight discoloration was observed, which it was exclusively related to adsorption process (absence of *OH - Figure 7a). Furthermore, the results showed that the Naβ has a higher adsorption capacity compared to NaY. This result is interesting since the surface area of the NaY is three times higher than the Naβ (Table 1), suggesting that the cavity size in the NaY prevents the entry of methylene blue molecules within the pores. In fact, Naβ features a majority mesoporous structure ($V_{Mesopores}$ = 0.25 $cm^3.g^{-1}$), while a microporous structure is predominant in the NaY ($V_{Mesopores}$ = 0.01 $cm^3.g^{-1}$).

The presence of Fe and Cu species in the modified zeolites increased considerably the velocity of removal of the methylene blue dye (Figure 7b). This effect is clearly observed for the catalysts β-Cu or β-Fe that showed a remarkable increase in the discoloration compared to Y-Cu and Y-Fe zeolites. According to the kinetics study for H_2O_2 decomposition, would be expected a higher activity for Y-Cu and β-Cu samples, owing to formation of very reactive *OH specie which is extremely efficient for oxidation of several organic substrate. Apparent discrepancy between H_2O_2 decomposition and oxidation kinetics results should addressed based on the mechanism and structure of zeolites. Although, Y-Cu was efficient for H_2O_2 degradation and *OH radical production, the methylene blue molecules cannot access the micropores. Taking into account that the *OH life-time is very short (high reactivity), there is not enough time to travel all the way toward the

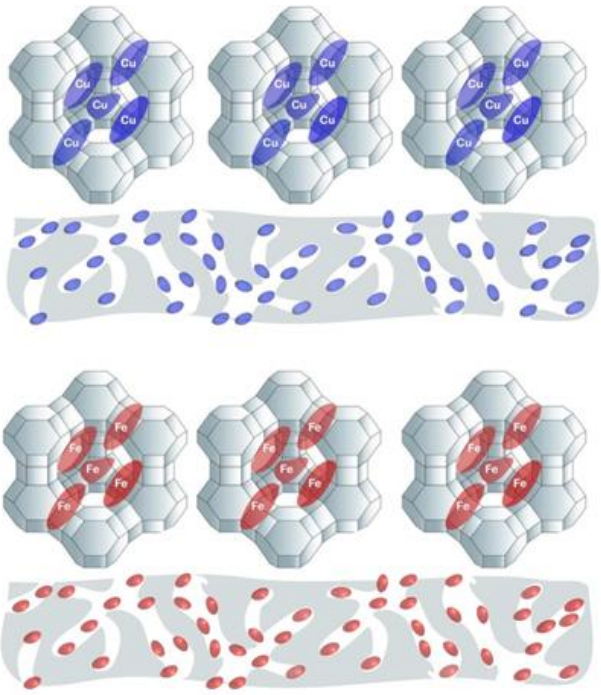

Figure 6. Schematic representation of the formation of copper and iron clusters within the pores of zeolites.

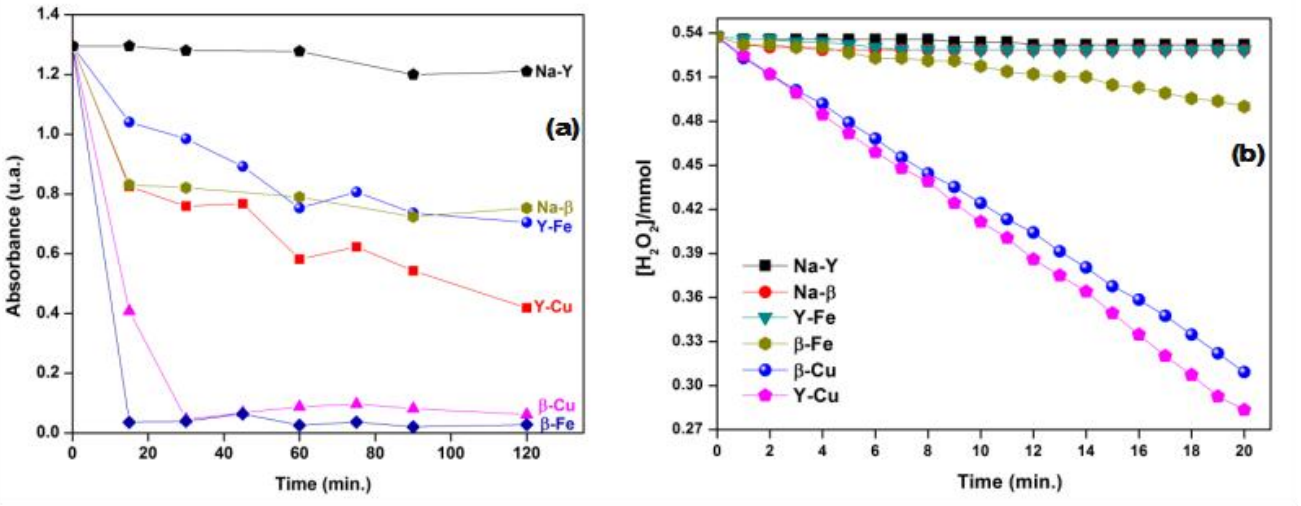

Figure 7. Kinetics studies for precursors and modified zeolites: (a) decomposition of H_2O_2 and (b) discoloration of methylene blue dye with H_2O_2

outside of the pores and attack the methylene blue molecules in solution. Thus, only the *OH radical produced on the surface and inside the pores in the macropores are effective in the methylene blue oxidation. On the contrary, β-Cu or β-Fe samples exhibit a mesoporous structure allowing the entry of methylene blue onto cavities, consequently, the dye can be readily oxidized.

Figure 8 shows the results obtained from the mass spectrometry analyzes, applying the ESI for the screening of the oxidized species formed during the oxidation reaction of methylene blue in the presence of the zeolites and H_2O_2.The ESI-MS spectrum obtained for the methylene blue dye solution shows only a strong signal at m/z = 284 (Figure 8a), related to the methylene blue ion. After 15 min of reaction with the Y-Cu and hydrogen peroxide, new signals appear at m/z = 300 and m/z = 316, as shown in Figure 8b, but, the signal of the dye (m/z = 284) is still intense. Figure 8c show the ESI-MS spectrum of the reaction after 15 min for the β-Cu catalyst. As can be observed the signal of the m/z = 284 was reduced below 20 % and a new signal with m/z = 130 appears in the spectrum which is related to the presence of intermediates of the methylene blue oxidation, suggesting that the structural ring of dye was somehow broken apart. Only a very small signal associated with m/z = 130 was noticed in the ESI-MS spectrum for dye solution in Y-Fe even after 60 minutes whereas the m/z = 284 remains close to 80% (Figure 8e**).** This result confirms that for this material the adsorption process is the main mechanism for removal dye. Conversely, for β-Fe strong signal with m/z = 130 about 90 % is clearly noticed while the signal related to methylene blue (m/z = 284) was reduced below 10 % after 10 minutes of reaction (Figure 8f**)**.

Figure 9 shows the proposed intermediate structures of the complete oxidation reaction pathway from methylene blue to CO_2 and H_2O. Based on the results from Figure 8 we could propose that the reaction initiated by the activation of H_2O_2 by zeolites was followed by the transference of *OH radical to organic dye as showed by the intense fragments. The proposed mechanism was based on the activation of H_2O_2 via a heterogeneous Fenton mechanism to form a radical *OH as suggested by ESI-MS data [2, 34].

It is worth to point out that the solutions after the heterogeneous Fenton reactions were submitted to elemental analysis using atomic absorption spectrometry (AAS) in order to investigate the possibility of homogeneous reactions owing to Cu and Fe ions lixiviation from modified zeolites. The results have not revealed the presence of Cu or Fe species in the solutions confirming the heterogeneous oxidation process.

4. Conclusion

In the presented study, we report a study of catalytic activity of the Y and β zeolites modified with iron or copper employing the ion exchange based preparation method in two reactions: (i) the H_2O_2 decomposition to O_2 ($H_2O_2 \rightarrow H_2O + 0.5O_2$); (ii) the oxidation of the model contaminant the methylene blue dye with H_2O_2 in aqueous medium. Ion-exchange method was used to

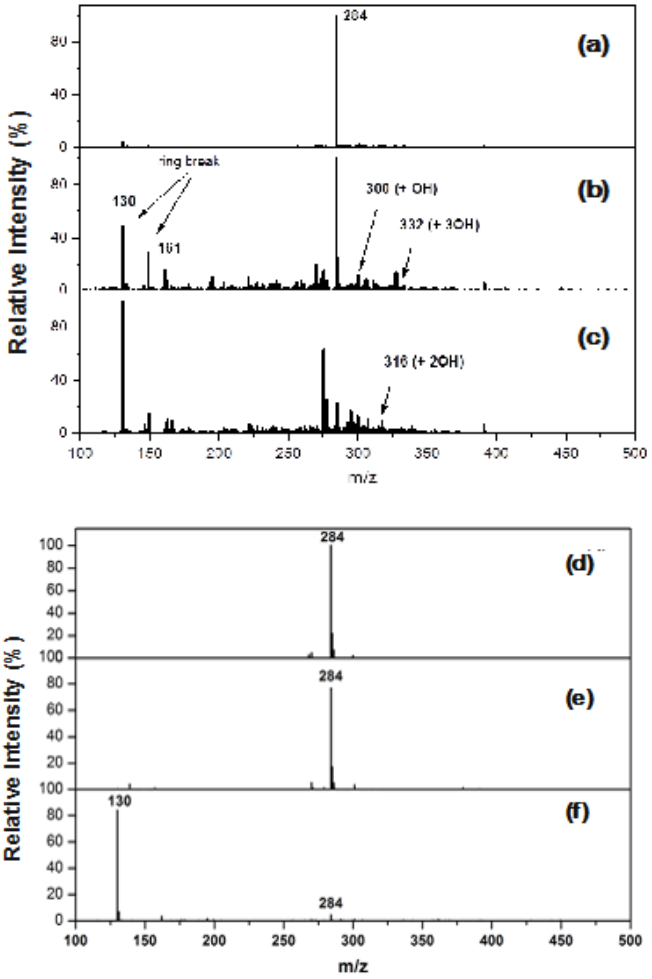

Figure 8. ESI mass spectra in the positive ion mode for monitoring the oxidation of methylene blue dye in water: (a) methylene blue dye water solution (100 ppm and m/z = 284) (without zeolite), (b) Y-Cu and (c) b-Cu in the presence of H_2O_2 for 15 min of reaction, (d) methylene blue dye water solution (10 ppm and m/z = 284) (without zeolite), (e) Y-Fe in the presence of H_2O_2 for 12 hours of reaction, and (f) b-Fe in the presence of H_2O_2 for 10 min of reaction.

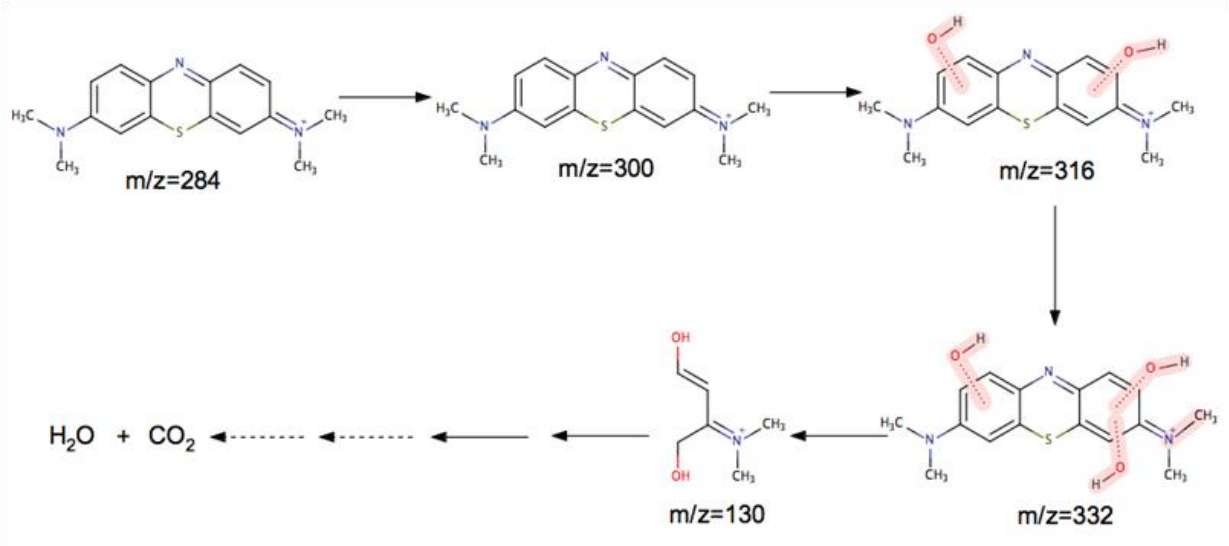

Figure 9. Scheme with intermediates proposed for the oxidation of methylene blue dye (m/z = 284) by the modified zeolites and H_2O_2 system

synthesize β-Fe and β-Cu mesoporous material catalysts and Y-Fe and Y-Cu microporous catalysts. X-ray powder diffraction results confirmed the authenticity and phase purity of β and Y zeolites. Regarding to the modified zeolites the occurrence of specific diffraction peaks characteristic of crystalline phases of copper or iron in the Y-Cu and Y-Fe samples is unclear. β-Fe, β-Cu, Y-Fe, and Y-Cu material exhibited decreased surface area compared to β and Y precursors. It was concluded that the reason for such a behavior of the modified zeolites was partial blockage of pores by iron or copper oxides. TPR experiments for β-Fe, β-Cu, Y-Fe, and Y-Cu revealed the presence of different Cu and Fe oxides. The β-Fe and β-Cu showed a remarkable activity in H_2O_2 decomposition and in the discoloration an organic dye in aqueous medium. The catalytic performance for Y-Fe, and Y-Cu zeolites was reduced owing to the characteristic microporous structure of Y zeolite. ESI-MS studies of the methylene blue oxidation showed that the oxidation of the dye occurs via a Fenton type system in which *OH radicals are formed in situ and added to the ring structure, suggesting that it is possible to reach the total mineralization of the organic substrate; not only its discoloration.

Acknowledgment

The authors are grateful to CAPES, CNPq, FAPEMIG and CAPQ-UFLA by financial support. The authors gratefully acknowledge the essential contributions of Professor Dr. Sibele Pergher and Chemical Institute of Technology in Valence for donation of zeolites.

References

[1] Nigam, P., Banat, I. M., Singh, D. & Marchant, R. (1996). Microbial process for the decolorization of textile effluent containing azo, diazo and reactive dyes. *Process Biochemistry*, 31: 435-442.

[2] Mishra, M. & Jain, S. K. (2011). Properties and applications of zeolites: A Review. *Proceedings of the National Academy of Sciences India Section B-Biological Sciences*, 81: 250-259.

[3] Hao, L., Wang, R., Fang, K., Liu, J., Sun, Y. & Men, Y. (2015). The synchronized wash-off of reactive-dyed cotton fabrics and decolorization of resultant wastewater using titanium dioxide nano-fibers. *Carbohydrate Polymers*, 125: 367-375.

[1] Chen, J., Wang, X., Liu, X., Huang, J. & Xie, Z. (2015). Removal of Dye Wastewater COD by Sludge Based Activated Carbon. *Journal of Coastal Research*: 1-3.

[2] Choudary, N. V. & Newalkar, B. L. (2011). Use of zeolites in petroleum refining and petrochemical processes: recent advances. *Journal of Porous Materials*, 18: 685-692.

[3] Oliveira, L. C. A., Goncalves, M., Guerreiro, M. C., Ramalho, T. C., Fabris, J. D., Pereira, M. C. & Sapag, K. (2007). A new catalyst material based on niobia/iron oxide composite on the oxidation of organic contaminants in water via heterogeneous Fenton mechanisms. *Applied Catalysis A: General*, 316: 117-124.

[4] Aboul-Gheit, A. K., Awadallah, A. E., Aboul-Enein, A. A. & Mahmoud, A. L. H. (2011). Molybdenum substitution by copper or zinc in H-ZSM-5 zeolite for catalyzing the direct conversion of natural gas to petrochemicals under non-oxidative conditions. *Fuel*, 90: 3040-3046.

[5] Forgacs, E., Cserhti, T. & Oros, G. (2004). Removal of synthetic dyes from wastewaters: a review. *Environment International*, 30: 953-971.

[6] Wang, X., Wang, P., Ma, J., Liu, H. & Ning, P. (2015). Synthesis, characterization, and reactivity of cellulose modified nano zero-valent iron for dye discoloration. *Applied Surface Science*, 345: 57-66.

[7] Gusmao, K. A. G., Gurgel, L. V. A., Melo, T. M. S. & Gil, L. F. (2012). Application of succinylated sugarcane bagasse as adsorbent to remove methylene blue and gentian violet from aqueous solutions - Kinetic and equilibrium studies. *Dyes and Pigments*, 92: 967-974.

[8] Gupta, V. K., Carrott, P. J. M., Carrott, M. M. L. R. & Suhas (2009). Low-Cost Adsorbents: Growing Approach to Wastewater Treatment Review. Critical *Reviews in Environmental Science and Technology*, 39: 783-842.

[9] Teketel, S., Skistad, W., Benard, S., Olsbye, U., Lillerud, K. P., Beato, P. & Svelle, S. (2012). Shape Selectivity in the Conversion of Methanol to Hydrocarbons: The Catalytic Performance of One-Dimensional 10-Ring Zeolites: ZSM-22, ZSM-23, ZSM-48, and EU-1. *ACS Catalysis*, 2: 26-37.

[10] Erten-Kaya, Y. & Cakicioglu-Ozkan, F. (2012). Effect of ultrasound on the kinetics of cation exchange in NaX zeolite. *Ultrasonics Sonochemistry*, 19: 701-706.

[11] Oliveira, L. C. A., Rios, R. V. R. A., Fabris, J. D., Sapag, K., Garg, V. K. & Lago, R. M. (2003). Clay, iron oxide magnetic composites for the adsorption of contaminants in water. *Applied Clay Science*, 22: 169-177.

[12] Ong, S. A., Toorisaka, E., Hirata, M. & Hano, T. (2005). Treatment of azo dye Orange II in aerobic and anaerobic-SBR systems. *Process Biochemistry*, 40: 2907-2914.

[13] Ding, L. H. & Zheng, Y. (2007). Nanocrystalline zeolite beta: The effect of template agent on crystal size. *Materials Research Bulletin*, 42: 584-590.

[14] Yang, R. T., Tharappiwattananon, N. & Long, R. Q. (1998). Ion-exchanged pillared clays for selective catalytic reduction of NO by ethylene in the presence of oxygen. *Applied Catalysis B: Environmental*, 19: 289-304.

[15] Oliveira, L. C. A., Petkowicz, D. I., Smaniotto, A. & Pergher, S. B. C. (2004). Magnetic zeolites: a new adsorbent for removal of metallic contaminants from water. *Water Research*, 38: 3699-3704.

[16] Mignoni, M. L., Detoni, C. & Pergher, S. B. C. (2007). Estudo da síntese da zeólita ZSM-5 a partir de argilas naturais. *Química Nova*, 30: 45-48.

[17] Baur, W. H. (1964). On the cation and water positions in faujasite. *Am. Miner.*, 49: 697-704.

[18] Alberti, A., Cruciani, G., Galli, E., Merlino, S., Millini, R., Quartieri, S., Vezzalini, G. & Zanardi, S. (2002). Crystal structure of tetragonal and monoclinic polytypes of tschernichite, the natural counterpart of synthetic zeolite beta. *Journal of Physical Chemistry B*, 106: 10277-10284.

[19] Treacy, M. M. J., Higgins, J. B. & vonBallmoos, R. (1996). Collection of simulated XRD powder patterns for zeolites. *Zeolites*, 16: 327-&.

[20] Li, B. X., Wang, X. F., Xia, D. D., Chu, Q. X., Liu, X. Y., Lu, F. G. & Zhao, X. D. (2011). One-step green synthesis of cuprous oxide crystals with truncated octahedra shapes via a high pressure flux approach. *Journal of Solid State Chemistry*, 184: 2097-2102.

[21] Iizumi, M., Koetzle, T. F., Shirane, G., Chikazumi, S., Matsui, M. & Todo, S. (1982). Structure of Magnetite (Fe3o4) Below the Verwey Transition-Temperature. *Acta Crystallography B*, 38: 2121-2133.

[22] Nogueira, F. G. E., Lopes, J. H., Silva, A. C., Lago, R. M., Fabris, J. D. & Oliveira, L. C. A. (2011). Catalysts based on clay and iron oxide for oxidation of toluene. *Applied Clay Science*, 51: 385-389.

[23] Peña, Y., Rondón, W. (2013). Linde Type a Zeolite and Type Y Faujasite as a Solid-Phase for Lead, Cadmium, Nickel and Cobalt Preconcentration and Determination Using a Flow Injection System Coupled to Flame Atomic Absorption Spectrometry. *American Journal of Analytical Chemistry*, 4(8): 387-397. doi: 10.4236/ajac.2013.48049

[24] A., T., S., R., B., P. G., Shankar K., R. S., M., R. & K., M. (2008). Trace Element Studies and Origin of Magnetite Quartzite Iron Formations of Northern District of Tamil Nadu, India. *Asian Journal of Applied Sciences*, 1: 327-333

[25] Padil, V. V. T. & Černík, M. (2013). Green synthesis of copper oxide nanoparticles using gum karaya as a biotemplate and their antibacterial application. *International Journal of Nanomedicine*, 8: 889-898.

[26] Urquieta-González, E. A., Martins, L., Peguin, R. P. S. & Batista, M. S. (2002). Identification of Extra-Framework Species on Fe/ZSM-5 and Cu/ZSM-5 Catalysts Typical Microporous Molecular Sieves with Zeolitic Structure. *Materials Research*, 5: 321-327.

[27] Bulanek, R., Wichterlova, B., Sobalik, Z. & Tichy, J. (2001). Reducibility and oxidation activity of Cu ions in zeolites - Effect of Cu ion coordination and zeolite framework composition. *Applied Catalysis B: Environmental*, 31: 13-25.

[28] Rac, V., Rakic, V., Gajinov, S., Dondur, V. & Auroux, A. (2006). Room-temperature interaction of n-hexane with ZSM-5 zeolites - Microcalorimetric and temperature-programmed desorption studies. *Journal of Thermal Analysis and Calorimetry*, 84: 239-245.

[29] Yang, Y. X., Burke, N., Zhang, J. F., Huang, S. L., Lim, S. & Zhu, Y. G. (2014). Influence of charge compensating cations on propane adsorption in X zeolites: experimental measurement and mathematical modeling. *RSC Advances*, 4: 7279-7287.

[30] Stanic, T., Dakovic, A., Zivanovic, A., Tomasevic-Canovic, M., Dondur, V. & Milicevic, S. (2009). Adsorption of arsenic (V) by iron (III)-modified natural zeolitic tuff. *Environmental Chemistry Letters*, 7: 161-166.

[31] Estermann, M., Mccusker, L. B., Baerlocher, C., Merrouche, A. & Kessler, H. (1991). A Synthetic Gallophosphate Molecular-Sieve with a 20-Tetrahedral-Atom Pore Opening. *Nature*, 352: 320-323.

Supplementary Materials

SM1. Morphology of zeolites by SEM microscopy

The zeolite morphology was probed by using a scanning electron microscope (Leo Electron Microscopy Inc., model LEO 1550, Thornwood, NY, USA). The applied acceleration voltage was 20 kV. In a preliminary step, the samples were attached to the specimen holder using a carbon tape and silver paste. At a later stage, the samples were coated with carbon and gold using a sputter (BALTEC Maschinenbau AG Med model 020, Pfaffikon, Switzerland) and analyzed by SEM.

The morphology of zeolites before and after the modification by SEM is presented in Figure SM-1. SEM pictures show morphology with hierarchical structure composed of aggregates of particles of various sizes and irregular shape. Actually, these agglomerates are aggregates of nanosized zeolite crystals with well-defined grain boundaries. Modified zeolites exhibit similar morphology of the precursors, composed of aggregates of zeolite nanoparticles.

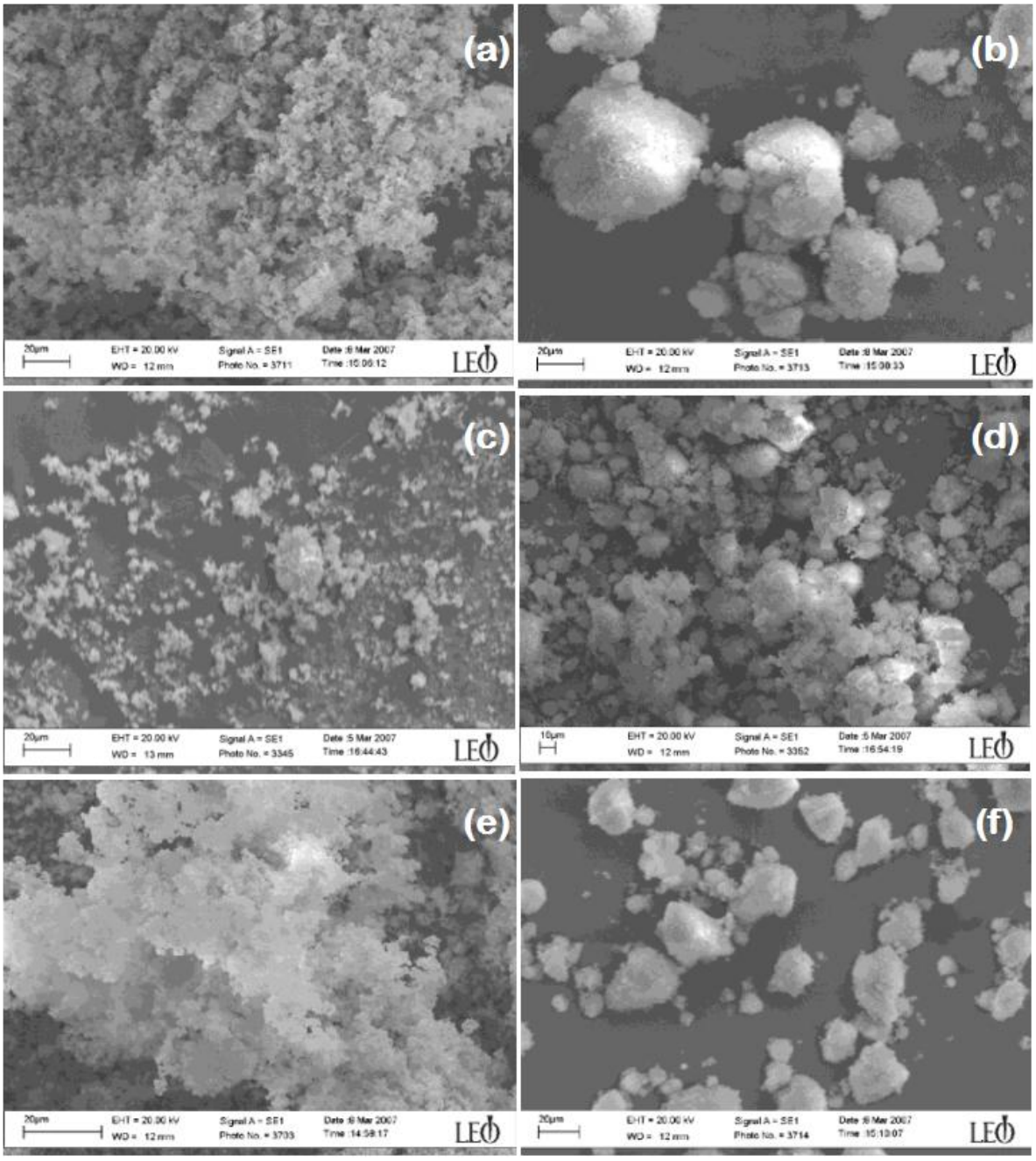

Figure SM-1. SEM micrographs of zeolites: (a) NaY, (b) Naβ, (c) NaY-Fe, (d) Naβ-Fe, (e) NaY-Cu, and (f) Naβ-Cu